Multiheme hydroxylamine oxidoreductases produce NO during ammonia oxidation in methanotrophs

Wouter Versantvoort[a], Arjan Pol[a], Mike S. M. Jetten[a], Laura van Niftrik[a], Joachim Reimann[a], Boran Kartal[b,1], and Huub J. M. Op den Camp[a]

[a]Department of Microbiology, Institute for Water and Wetland Research, Faculty of Science, Radboud University, 6525 AJ Nijmegen, The Netherlands; and [b]Microbial Physiology Group, Max Planck Institute for Marine Microbiology, 28359 Bremen, Germany

Edited by Caroline S. Harwood, University of Washington, Seattle, WA, and approved August 6, 2020 (received for review June 2, 2020)

Aerobic and nitrite-dependent methanotrophs make a living from oxidizing methane via methanol to carbon dioxide. In addition, these microorganisms cometabolize ammonia due to its structural similarities to methane. The first step in both of these processes is catalyzed by methane monooxygenase, which converts methane or ammonia into methanol or hydroxylamine, respectively. Methanotrophs use methanol for energy conservation, whereas toxic hydroxylamine is a potent inhibitor that needs to be rapidly removed. It is suggested that many methanotrophs encode a hydroxylamine oxidoreductase (mHAO) in their genome to remove hydroxylamine, although biochemical evidence for this is lacking. HAOs also play a crucial role in the metabolism of aerobic and anaerobic ammonia oxidizers by converting hydroxylamine to nitric oxide (NO). Here, we purified an HAO from the thermophilic verrucomicrobial methanotroph *Methylacidiphilum fumariolicum* SolV and characterized its kinetic properties. This mHAO possesses the characteristic P_{460} chromophore and is active up to at least 80 °C. It catalyzes the rapid oxidation of hydroxylamine to NO. In methanotrophs, mHAO efficiently removes hydroxylamine, which severely inhibits calcium-dependent, and as we show here, lanthanide-dependent methanol dehydrogenases, which are more prevalent in the environment. Our results indicate that mHAO allows methanotrophs to thrive under high ammonia concentrations in natural and engineered ecosystems, such as those observed in rice paddy fields, landfills, or volcanic mud pots, by preventing the accumulation of inhibitory hydroxylamine. Under oxic conditions, methanotrophs mainly oxidize ammonia to nitrite, whereas in hypoxic and anoxic environments reduction of both ammonia-derived nitrite and NO could lead to nitrous oxide (N_2O) production.

hydroxylamine oxidoreductase | ammonia oxidation | methanotrophy | multiheme cytochrome | nitric oxide

Methane (CH_4) is a potent greenhouse gas with a global warming potential 34 times that of carbon dioxide (CO_2) over a 100-y time span (1). Microbial anaerobic degradation of biomass yields organic acids and hydrogen that fuel methanogenesis. Methanogenic archaea are responsible for the production of the majority of biogenic methane (about 583 $Tg \cdot y^{-1}$) (2), which is subsequently released to the environment. Emission of this methane to the atmosphere is partly mitigated by aerobic and anaerobic methanotrophs (3). These microorganisms use methane as an energy source by oxidizing it to CO_2 and act as a methane sink, thereby reducing the contribution of methane on global warming. On the other hand, aerobic and nitrite-dependent methanotrophs can be the source of another, even more potent greenhouse gas, nitrous oxide (N_2O), which has a global warming potential 296 times that of CO_2 over a 100-y time span (1, 4). According to the Fifth Assessment Report of the Intergovernmental Panel on Climate Change, the total radiative forcing of CH_4 and N_2O increased by 2% and 6%, respectively, since the previous report (1). This increase makes N_2O the third largest contributor to radiative forcing. Furthermore, since the chlorofluorocarbons were phased out of use, N_2O became the primary ozone-depleting greenhouse gas (5). Consequently, methanotrophs sit in the nexus of both carbon and nitrogen cycles and can act both as sources and sinks of climate active gases. Therefore, understanding their metabolism and how this is influenced by anthropogenic activities will help us predict their effect on global warming and possibly utilize them to counteract emissions (6–10).

Ammonia oxidation in the natural environment has been mainly attributed to a distinct group of microorganisms, termed ammonia oxidizers (11, 12). However, in natural and engineered environments where methane and ammonia co-occur, methanotrophs can also contribute significantly to ammonia oxidation (8, 9, 13–17).This cross-reactivity is due to the structural similarity between methane and ammonia, which allows both methanotrophs and ammonia oxidizers to convert either substrate, although neither is capable of growing on the alternative substrate (4, 9, 17). The first step in both methane and ammonia oxidation is the incorporation of oxygen by methane/ammonia monooxygenase (MMO, AMO), resulting in the formation of methanol or hydroxylamine, respectively (4, 17–19). In methane-oxidizing bacteria, methanol dehydrogenase (MDH) converts methanol to formaldehyde (or formate), which is further oxidized to CO_2 (6, 20, 21). Whereas in ammonia-oxidizing microorganisms, hydroxylamine oxidoreductase (HAO) oxidizes hydroxylamine to nitric oxide (NO), which is subsequently converted to nitrite (22–24). In octaheme HAO proteins catalysis occurs at heme 4, which is cross-linked to a tyrosine residue from a neighboring subunit, covalently linking all three subunits of the HAO complex (22, 25–29). This cross-link forces the heme into a

Significance

Methanotrophs oxidize methane to CO_2, thereby mitigating the emission of this potent greenhouse gas. Understanding how these microorganisms are influenced by anthropogenic activities will help better predict their impact on global warming and utilize them to reduce it. Ammonia-fertilizer input to the environment has greatly improved crop yields but increased emissions of greenhouse gasses like N_2O as well. In methane-rich environments, methanotrophs play a prominent role in ammonia oxidation. Here, we purified a protein (mHAO) from *Methylacidiphilum fumariolicum*, capable of rapid oxidation of hydroxylamine to NO. We propose that mHAO enables methanotrophs to cope with high ammonia concentrations, leading to reduced methane emissions. However, this activity simultaneously contributes to ammonia loss and nitrite production, and potentially leads to N_2O emissions.

Author contributions: W.V., A.P., J.R., B.K., and H.J.M.O.d.C. designed research; W.V. and A.P. performed research; W.V., A.P., M.S.M.J., L.v.N., J.R., B.K., and H.J.M.O.d.C. analyzed data; and W.V. and B.K. wrote the paper.

The authors declare no competing interest.

This article is a PNAS Direct Submission.

[1]To whom correspondence may be addressed. Email: bkartal@mpi-bremen.de.

This article contains supporting information online at https://www.pnas.org/lookup/suppl/doi:10.1073/pnas.2011299117/-/DCSupplemental.

First published September 10, 2020.

highly ruffled conformation, giving rise to the characteristic absorbance peak at 460 nm (P_{460}) in the reduced enzyme (26, 27). The active site of HAOs strongly favors oxidative reactions and the cross-linking tyrosine is highly conserved within members of the HAO family (28).

Hydroxylamine is a highly toxic compound and has been shown to inhibit calcium-dependent MDHs (30), which necessitates the rapid turnover of hydroxylamine in methane-oxidizing bacteria. Many methanotrophs encode a HAO-like protein (mHAO) homologous to that of bacterial ammonia oxidizers. These HAO-like proteins have been postulated to perform hydroxylamine oxidation in methanotrophs, but biochemical evidence for this is lacking (4). Up-regulation of *hao* transcription in response to ammonia has been shown for several methanotrophic bacteria that oxidize ammonia faster compared to the ones not encoding *hao* genes (31–34). Most cultured methanotrophs oxidize ammonium to nitrite (17, 33–35), whereas a few methanotrophs have been shown to produce N_2O from ammonia oxidation without apparent nitrite production (36). In addition, N_2O production has been observed for many aerobic methanotrophs under nitrite-reducing conditions, either as a product of reactive nitrogen detoxification or respiration under O_2 limitation (31, 34, 36–38). N_2O production from ammonia and hydroxylamine is thought to occur via the initial formation of nitrite, which until recently was the presumed end product of hydroxylamine oxidation by all HAOs. In this hypothesis, nitrite reductases *nirS* and *nirK* would produce NO, which would subsequently be reduced to N_2O by a *norBC* complex (29, 31–34). However, the close amino acid sequence similarity of the mHAO proteins to those encoded by ammonia-oxidizing bacteria suggests that the end product of mHAO could also be NO (27, 28). Thus, NO would be produced as an obligate intermediate in ammonia oxidation by methanotrophs as well.

To date, there is no biochemical evidence for the role of these HAO-like proteins in hydroxylamine oxidation in methanotrophic bacteria. Here, we present the purification of an mHAO protein from the verrucomicrobial thermoacidiphilic methanotroph *Methylacidiphilum fumariolicum* SolV (39). We studied the catalytic properties of this methanotroph HAO and compared it to its homologs from both aerobic and anaerobic ammonia oxidizers. We suggest that mHAO has a crucial role in preventing the hydroxylamine inhibition of MDH, and help methanotrophs thrive in environments where methane and ammonia coexist.

Results

mHAO Catalyzes the Oxidation of Hydroxylamine to NO. *M. fumariolicum* SolV encodes an HAO-like protein with an N-terminal fusion to a monoheme cytochrome *c* in its genome (*haoA*, Mfumv2_2472). The molecular mass of a single subunit of this protein is 83,860 Da including the protein backbone and 9 heme *c* moieties, excluding the signal peptide. Multiple sequence alignment of this protein with other HAO-like proteins from both aerobic and anaerobic ammonia oxidizers and methanotrophs (*SI Appendix*, Fig. S1) showed that heme spacing and the cross-linking tyrosine were conserved among all analyzed proteins. This tyrosine (TYR467, numbering of NeHAO) (26) covalently binds the three HAO monomers. To examine whether this HAO-like protein from *M. fumariolicum* SolV is a bona fide HAO, capable of oxidizing hydroxylamine, the enzyme was purified to homogeneity by a two-step column chromatography procedure. As observed for HAO-like proteins with the tyrosine cross-link (27, 40), the purified enzyme showed two bands on a denaturing SDS/PAGE, both of which had a dominant heme stain signal (*SI Appendix*, Fig. S2*A*). Both SDS/PAGE bands were identified as the gene product of Mfumv2_2472 (*haoA)* by matrix-assisted laser desorption/ionization time-of-flight mass spectrometry (MALDI-TOF MS). On a nondenaturing clear native PAGE, a band at 500 kDa and a band at 250 kDa were observed (*SI Appendix*, Fig. S2*B*). Both bands were stained with an in-gel hydroxylamine oxidation stain. The UV-vis spectrum of purified mHAO displayed a prominent maximum at 468 nm in the reduced form. In addition, characteristic heme *c* features, namely a maximum in the Soret region at 408 nm in the oxidized form (Fig. 1, solid) and maxima at 418 nm for the Soret and 522 and 551 nm for the beta and alpha bands, respectively (Fig. 1, dashed) were observed. Activity assays with bovine cytochrome *c* as electron acceptor showed that mHAO catalyzed the rapid oxidation of hydroxylamine with a V_{max} of 5.5 ± 0.1 μmol·min^{-1}·mg protein^{-1}, K_m of 1.4 ± 0.1 μM, and a K_{cat} of 7.2 ± 0.15 s^{-1} (Table 1).

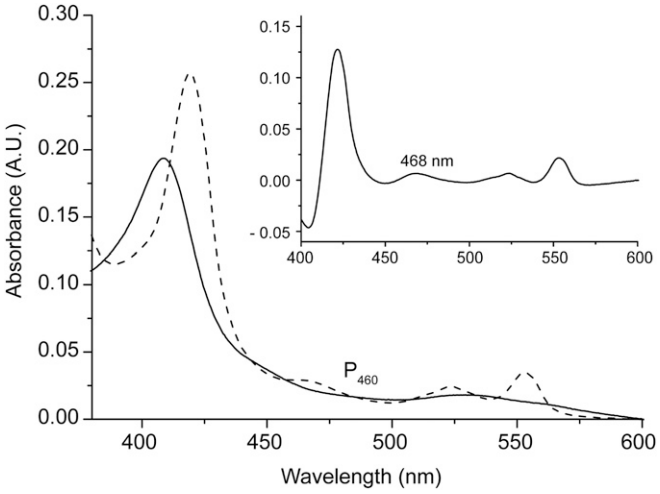

Fig. 1. UV-vis absorbance spectrum of *Methylacidiphilum fumariolicum* SolV HAO in the as-isolated (solid) and dithionite reduced state (dashed). *Inset* shows the reduced minus oxidized difference spectrum. The P_{460} chromophore characteristic for HAOs is clearly present in both the reduced and reduced minus oxidized difference spectrum.

To determine the end-product of hydroxylamine oxidation by mHAO, two different methods were employed. First, the production of NO from hydroxylamine by mHAO was examined using membrane inlet mass spectrometry (MIMS). In the absence of oxygen, mHAO catalyzed the stoichiometric conversion of hydroxylamine to NO with a recovery rate of 94 ± 4% of the added hydroxylamine as NO (Fig. 2*A*). The production of NO was corroborated by following the reduction of bovine cytochrome *c* by mHAO with a limiting amount of hydroxylamine (Fig. 2*B*). Here, the electron stoichiometry of hydroxylamine oxidation was determined to be 3 to 1 (3 ± 0.06 μM of reduced cytochrome *c* per μM hydroxylamine) indicating the formation of NO (Eq. **1**). These results were in line with recent studies that established NO to be the product of hydroxylamine oxidation by HAO enzymes (27, 29):

$$NH_2OH \rightarrow NO + 3e^- + 3H^+. \quad [1]$$

mHAO Is Tuned to Higher Temperature. The temperature dependence of hydroxylamine oxidation by mHAO and its homolog from the anaerobic ammonium oxidizing bacterium *Kuenenia stuttgartiensis* (KsHAO) were investigated in the range of 20 to 80 °C (Fig. 3). KsHAO showed a temperature optimum at 50 °C and was no longer active at temperatures above 60 °C. mHAO showed a temperature optimum at 60 °C and maintained ~80% of its maximum activity at temperatures above 60 °C. The rapid decomposition of hydroxylamine at higher temperatures prohibited activity measurements above 80 °C.

XoxF-Type MDH Is Inhibited by Hydroxylamine. *M. fumariolicum* SolV encodes for a lanthanide-dependent XoxF-type MDH, which was

Table 1. Kinetic parameters of *Methylacidiphilum fumariolicum* SolV HAO (mHAO) compared to its characterized homologs from *Kuenenia stuttgartiensis* (KsHAO) and *Nitrosomonas europaea* (NeHAO)

Enzyme	mHAO*	KsHAO†	NeHAO‡
V_{max}, μmol $NH_2OH \cdot min^{-1} \cdot mg\ HAO^{-1}$	5.5	4.8	9.5
K_m, μM	1.4	4.4	3.6
K_{cat}, s^{-1}	7.2	4.9	10.5
K_{cat}/K_m, $s^{-1} \cdot \mu M^{-1}$	5.1	1.1	2.9

*pH 7.5, 60 °C.
†pH 7.0, 37 °C; values calculated from data presented by Maalcke et al. (27).
‡pH 9.5, room temperature; values calculated from data presented by Hooper and Nason (22).

purified directly from native biomass according to Pol et al. (41). To determine whether this enzyme is inhibited by hydroxylamine, as observed for the calcium-dependent MDH (30), methanol oxidation activity was assayed with various concentrations of hydroxylamine (0 to 100 μM) (*SI Appendix*, Fig. S3). Hydroxylamine was found to be a potent inhibitor (K_i = 0.52 ± 0.3 μM) of methanol oxidation by *M. fumariolicum* SolV XoxF-type MDH.

Discussion

Aerobic and nitrite-dependent methanotrophs cometabolize ammonia and produce hydroxylamine. This is similar to aerobic ammonia-oxidizing microorganisms, which encode HAO proteins to further oxidize hydroxylamine to NO. Likewise, methanotrophs require a pathway to oxidize hydroxylamine, since it has been shown to be a potent inhibitor of calcium-dependent MDH (K_i = 12 μM) (30). Here, we showed that the lanthanide-dependent MDH encoded by *M. fumariolicum* SolV was severely inhibited by hydroxylamine as well, with an inhibition constant of K_i = 0.5 μM. Recent environmental surveys revealed that lanthanide-dependent MDHs are prevalent and widespread in nature compared to the calcium-dependent MDHs (42). Consequently, the inhibition of lanthanide-dependent MDHs by hydroxylamine has an extensive impact, affecting environmentally relevant aerobic and nitrite-dependent methane oxidizers, which are both oxygen dependent (10, 43, 44), and highlighting the importance of HAO in these methanotrophs.

Based on the transcriptional up-regulation of *hao-like* genes in response to ammonia, and the susceptibility of methanotrophic strains lacking *hao* genes to ammonia, it has been postulated that HAO-like proteins are also involved in hydroxylamine oxidation in methanotrophs, although biochemical evidence for this is lacking (31, 32, 34). Here, we purified an HAO-like protein from the aerobic methanotroph *M. fumariolicum* SolV. Similar to other bona fide HAOs (22, 25–27, 29), mHAO contained a P_{460} chromophore, characteristic of HAOs involved in oxidative reactions (28). mHAO oxidized hydroxylamine rapidly (V_{max} = 5.5 μmol·min^{-1}·mg $protein^{-1}$, K_m = 1.4 μM, K_{cat} = 7.2 s^{-1}) and produced NO, as was recently demonstrated for aerobic and anaerobic ammonia-oxidizing bacteria (27, 29). The mHAO kinetic parameters were in the same order of magnitude as those observed for previously characterized ammonia oxidizer HAOs (22, 27), indicating that mHAO was an efficient hydroxylamine-oxidizing enzyme. Considering all secondary structure elements were conserved among the different mHAO sequences, it is highly likely that mHAO is involved in hydroxylamine oxidation in all oxygen-dependent methanotrophs.

In aerobic ammonia-oxidizing bacteria, the concerted activity of ammonia monooxygenase (AMO) and HAO convert ammonia to NO. These microorganisms primarily oxidize the produced NO to nitrite contributing to energy conservation via a hitherto-unknown NO-oxidizing enzyme (24). Essentially, the same pathway also occurs in oxygen-dependent methanotrophs, where methane monooxygenase and mHAOs convert ammonia via hydroxylamine to NO. How the produced NO is further converted could differ in distinct aerobic and nitrite-dependent methanotrophs. Many isolated aerobic methanotrophs, similar to aerobic ammonia oxidizers, produce nitrite as the end product of their ammonia-oxidizing activity (31–35), where we now show that NO is also an obligate free intermediate. Consequently, both clades of microorganisms would require an NO-oxidizing enzyme. Although the exact nature of this enzyme remains unknown, it is tempting to speculate that such an enzyme could be another shared feature in the nitrogen metabolism of ammonia- and methane-oxidizing microorganisms. Using the set of proteins they encode for ammonia oxidation to nitrite, known aerobic methanotrophs would be unable to grow, since they lack the hydroxylamine-ubiquinone reduction module that would couple this oxidation activity to energy conservation (4). In contrast to most cultured aerobic methanotrophs, conversion of ammonia to N_2O without external nitrite addition or detection of intermediary nitrite production has been shown in 14 strains of *Methylomonas methanica*, *Methylomonas koyamae*, and *Methylomonas lenta* (36). In these microorganisms, it is conceivable that instead of being first oxidized to nitrite, NO could be directly reduced to N_2O by an NO reductase, which is encoded by many methanotrophs (4, 31). Next to bona fide aerobic methanotrophs, also nitrite-dependent methane-oxidizing bacteria encode mHAO proteins (44, 45). These microorganisms use NO to produce their own oxygen, which they then use to active methane (45). Here, ammonia oxidation could potentially serve as an alternative source of NO, and could contribute to energy conservation and growth in nitrite-dependent methanotrophs.

Environmental ammonium concentrations up to 28 mM and temperatures up to 70 °C are found in volcanic mud pots, which are the natural habitat of *M. fumariolicum* (39, 46). In agreement with this, mHAO of *M. fumariolicum* is very thermostable, maintaining 80% of its maximum activity to at least 80 °C, compared to the HAOs of mesophilic ammonia oxidizers, which are nearly completely inactive above 60 °C (22). This enables *M. fumariolicum* to prevent hydroxylamine inhibition in its ammonia-rich natural environment, which lack an apparent bona fide ammonia-oxidizing

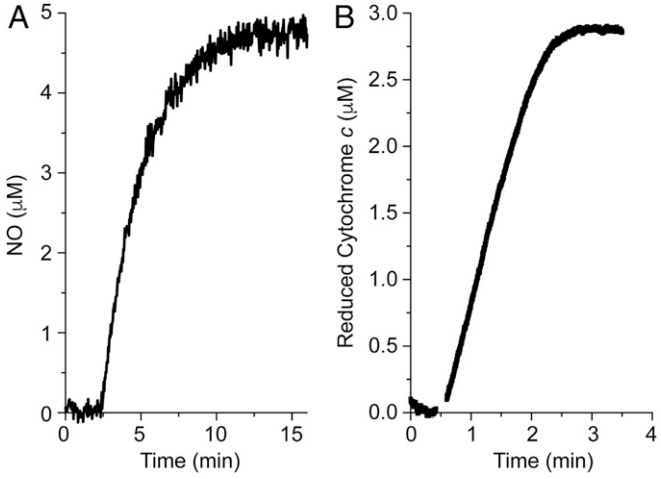

Fig. 2. NO production by mHAO from *Methylacidiphilum fumariolicum* SolV. (*A*) Sample trace of NO production by mHAO from 5 μM NH_2OH measured with membrane inlet mass spectrometry (MIMS). Hydroxylamine oxidation assays by mHAO with varying concentrations of hydroxylamine (2 to 5 μM), resulting in a recovery rate of 94 ± 4% (n = 6) of NO compared to the added amount of hydroxylamine. (*B*) Sample trace of cytochrome *c* reduction by mHAO with hydroxylamine. Addition of 1 μM hydroxylamine resulted in the reduction of 3 ± 0.06 μM (n = 3) cytochrome *c*, indicating the three-electron oxidation of hydroxylamine to NO by mHAO.

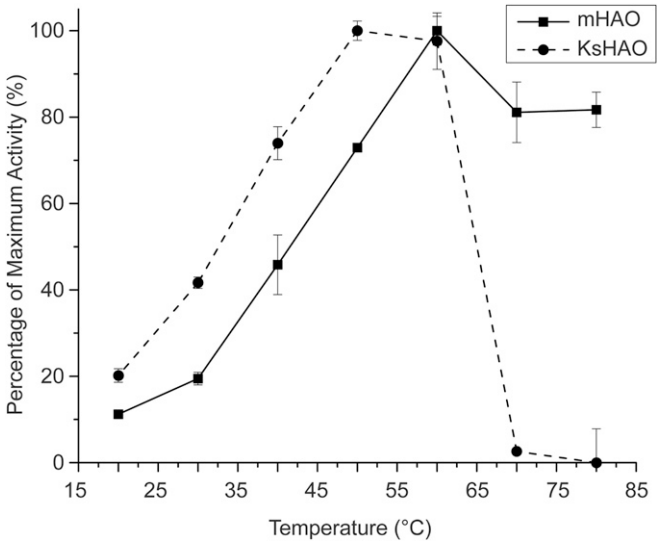

Fig. 3. Temperature dependence of mHAO from *Methylacidiphilum fumariolicum* SolV (solid) and KsHAO from *Kuenenia stuttgartiensis* (dashed) expressed as a percentage of the maximum activity ($n = 3$ per temperature; bars represent SD). The temperature dependence for mHAO is shifted by 10 °C compared to KsHAO. Activity of KsHAO is almost completely abolished at temperatures above 60 °C, whereas mHAO retains 80% of its activity at these temperatures.

microorganism. Next to volcanic mud pots, oxygen-dependent methane oxidizers commonly occur in other methane- and ammonia-rich ecosystems such as freshwater lakes, marine sediments, rice paddy fields, and landfills (7, 8, 13–15, 17, 43, 47, 48). In such environments, the multiheme mHAO, which is encoded by many methanotrophs, facilitates methane oxidizers to act as ammonia oxidizers.

Materials and Methods

Unless otherwise noted, all chemicals were purchased from VWR Chemicals (VWR International).

Growth of *Methylacidiphilum fumariolicum* SolV. *Methylacidiphilum fumariolicum* SolV (39) used in this study was cultured in a 10-L chemostat (Applikon). The growth medium, previously described by Pol et al. (41), was supplemented with 200 mM methanol. Methane was provided at a flow rate of 56 mL·min^{-1} via a mass flow controller. The reactor was kept at an oxygen concentration of ~1% by adjusting the flow rate of air via a mass flow controller in a feedback loop, using an oxygen probe connected to a Biocontroller (Applikon). After an OD_{600} of 1 was obtained, the pH of the reactor was gradually increased from pH 2.7 to pH 5 through the stepwise addition of 2 M NH_3, resulting in a final NH_4^+ concentration of 20 mM in the reactor. When the reactor reached a stable state at an OD_{600} of 5, a 6 mL·min^{-1} bleed was started, which was collected in a refrigerated bottle at 4 °C. Harvested cells were concentrated, washed once with ultrapure water (Merck-Millipore), and stored at −20 °C.

mHAO Purification. Frozen cell pellets were thawed and resuspended in 20 mM potassium phosphate buffer, pH 7. After breaking the cells by passing them three times through a French press (American Instrument Company) at 20,000 psi, cell debris and unbroken cells were removed by centrifugation at 10,000 × *g*, 4 °C for 1 h (Sorvall LYNX 4000, F12-6 × 500 LEX Fiberlite rotor; Thermo Fisher Scientific). The resulting supernatant was subjected to ultracentrifugation (Optima XE90; Beckman Coulter) at 160,000 × *g*, 4 °C, for 1 h in a fixed angle 45 Ti rotor (Beckman Coulter) to separate the soluble and membrane fraction. The soluble fraction was loaded onto a SP Sepharose-FF column (XK26/20; GE Healthcare) equilibrated with 20 mM potassium phosphate, 1 mM methanol, pH 7.2, and after washing, proteins were eluted using a linear gradient from 0 to 500 mM NaCl in 7 column volumes. Fractions containing hydroxylamine oxidizing activity were pooled, concentrated using 100-kDa cutoff spin filters (Vivaspin; Sartorius Stedim Biotech), and loaded onto a Superdex 200 size-exclusion column (GE Healthcare) equilibrated in 20 mM potassium phosphate, 1 mM methanol, 200 mM NaCl, pH 7.2. Fractions containing pure mHAO were pooled, concentrated, and stored at −80 °C until use. HAO from the anammox bacterium *Kuenenia stuttgartiensis* (KsHAO) was purified according to Maalcke et al. (27). All column chromatography was performed on an Äkta explorer FPLC system (GE Healthcare).

Enzyme Assays. Hydroxylamine oxidation was assayed following the reduction of bovine heart cytochrome *c* (Sigma-Aldrich) spectroscopically at 550 nm ($\Delta\varepsilon_{550}$ = 19.6 mM^{-1}·cm^{-1}) using a Cary 60 spectrophotometer (Agilent) in a 1-cm path length Suprasil quartz cuvette (Hellma). Assays were performed in 50 mM sodium phosphate, 50 mM NaCl, pH 7.5, with 50 μM cytochrome *c* and 1 to 1,000 μM hydroxylamine (Sigma-Aldrich). After establishing a baseline, the reaction was started through the addition of 3 nM mHAO or KsHAO. To determine the optimal temperature, a range of 20 to 80 °C was investigated at 100 μM hydroxylamine concentrations. To determine the kinetic parameters, the temperature was kept constant at the previously determined optimum of 60 °C, and hydroxylamine concentrations were varied between 1 and 1,000 μM. All measurements were performed in triplicate, and reaction rates were determined from the initial linear portion of the curve using the Cary 60 software. Kinetics were determined by fitting the initial reaction rates, corrected for chemical background rates, to Michaelis–Menten equations using Origin 9.1 (OriginLab). Specific activities were calculated based on the mHAO concentrations in the sample, calculated using the absorbance of the P_{460} ($\Delta\varepsilon_{468}$ = 58.7 mM^{-1}·cm^{-1}). To determine the electron stoichiometry of hydroxylamine oxidation, the reaction was followed to completion and the amount of reduced cytochrome *c* per mole hydroxylamine was calculated (27).

MDH activity assays were performed in duplicates using 20 mM potassium phosphate, pH 7.2, with 1 mM KCN, 1 mM phenazine ethosulfate (Sigma-Aldrich), 200 μM 2,6-dichlorophenolindophenol (DCPIP) (Sigma-Aldrich), 0 to 100 μM methanol (HPLC grade; JT-Baker), and 0 to 100 μM hydroxylamine at 45 °C. Methanol oxidation was followed by measuring the reduction of DCPIP spectroscopically at 600 nm (ε_{600} = 18.5 mM^{-1}·cm^{-1}) in a SpectraMax 190 plate reader (Molecular Devices). After establishing a stable baseline, reactions were started by the addition of 1 μM La-dependent MDH purified as described before (41). Kinetic parameters and the inhibition constant for hydroxylamine were determined by fitting the initial rates to a competitive enzyme-inhibition model using Origin 9.1 (OriginLab).

Membrane Inlet MS. Liquid concentrations of NO were measured with a Membrane Inlet Mass Spectrometer (HPR40, positive ion counting detector; Hiden Analytical) in a 10-mL chamber. Setup of the MIMS, MIMS chamber, and MIMS probe were done as described previously by Schmitz et al. (49). Assays were performed in 10 mM Hepes, pH 7, with 100 μM phenazine methosulfate (PMS) as electron acceptor and 2 to 5 μM hydroxylamine at 45 °C. The NO signal was calibrated by flushing the liquid using a 4% NO in He gas bottle with a flow of 10 mL/min.

UV-Vis Spectroscopy. UV-vis absorbance spectra in the range of 350 to 600 nm were measured in a 1-cm path length Suprasil quartz cuvette (Hellma) using a Cary 60 spectrophotometer (Agilent) in an anaerobic glove box. After recording an as-isolated spectrum (fully oxidized), protein was reduced by the addition of a few grains of sodium dithionite and another spectrum was recorded. The ratio of P_{460} to 550 nm varied between preparations. Since the P_{460} optical feature reports the active HAO population, the amount of HAO in the different preparations was determined using the extinction coefficient of the P_{460} ($\Delta\varepsilon_{468}$ = 58.7 mM^{-1}·cm^{-1}), determined based on KsHAO (27).

Gel Electrophoresis. To assess the purity of mHAO during purification, polyacrylamide gel electrophoresis was routinely applied. Acrylamide gradient gels (4 to 15%) were cast using a model 475 gradient delivery system (Bio-Rad). Denaturing gels were run and stained for protein and heme as adapted from previously described protocols (50, 51) using a Precision Plus Protein Dual Color standard (Bio-Rad) for molecular mass estimation. HrCN-1 gels were run according to the protocol described by Wittig et al. (52) using NativeMark Unstained protein standard (Thermo Fisher Scientific) for molecular mass estimation. Afterward, the gel was stained with Coomassie Brilliant Blue or with an in-gel hydroxylamine oxidation stain. The gel was incubated for 10 min in 20 mM potassium phosphate, pH 7, with 1 mM nitro blue tetrazolium (Sigma-Aldrich), after which 100 μM hydroxylamine was added. The gel was incubated at 50 °C until the stain was developed and then washed three times with ultrapure water.

MALDI-TOF MS. To identify proteins, MALDI-TOF MS analysis of tryptically digested peptides was performed as previously described (53). Spectra in the range of 600 to 3,000 *m/z* were collected using a Microflex LRF MALDI-TOF

(Bruker Daltonic) and analyzed using the Mascot Peptide mass Fingerprint program against the *Methylacidiphilum fumariolicum* SolV protein database, with a peptide tolerance of 0.3 Da, allowance of one missed cleavage and methionine oxidation as a variable modification.

Sequence Analysis. HAO sequences of various methanotrophs, *Kuenenia stuttgartiensis* and *Nitrosomonas europaea*, were downloaded from National Center for Biotechnology Information. Prediction and cleavage of signal peptides were performed with SignalP 5.0 (54). Multiple sequence alignment using the MUSCLE algorithm (55) was performed with MEGA X (56).

Data Availability Statement. All study data are included in the article and *SI Appendix*.

ACKNOWLEDGMENTS. W.V., J.R., and M.S.M.J. were supported by the European Research Council (ERC) Advanced Grant (AG) Ecomom 339880. W.V. was also supported by Netherlands Organization for Scientific Research (NWO) Grant 824.15.011 (to B.K.). L.v.N. was supported by NWO Grant VI.Vidi.192.001. H.J.M.O.d.C. was supported by ERC AG VOLCANO 669371. B.K. was supported by ERC Starting Grant GreenT 640422. We thank Christina Ferousi for providing KsHAO, and Bram Vekeman, Jana Milucka, and Katharina Ettwig for critically reading the manuscript.

1. G. Myhre *et al*., "Anthropogenic and natural radiative forcing" in *Climate Change 2013—The Physical Science Basis*, T. F. Stocker *et al*., Eds. (Cambridge University Press, Cambridge, UK, 2013), chap. 8, pp. 659–740.
2. M. Saunois *et al*., The global methane budget 2000–2012. *Earth Syst. Sci. Data* **8**, 697–751 (2016).
3. A. Y. Kallistova, A. Y. Merkel, I. Y. Tarnovetskii, N. V. Pimenov, Methane formation and oxidation by prokaryotes. *Microbiology* **86**, 671–691 (2017).
4. L. Y. Stein, M. G. Klotz, Nitrifying and denitrifying pathways of methanotrophic bacteria. *Biochem. Soc. Trans.* **39**, 1826–1831 (2011).
5. A. R. Ravishankara, J. S. Daniel, R. W. Portmann, Nitrous oxide (N_2O): The dominant ozone-depleting substance emitted in the 21st century. *Science* **326**, 123–125 (2009).
6. R. S. Hanson, T. E. Hanson, Methanotrophic bacteria. *Microbiol. Rev.* **60**, 439–471 (1996).
7. P. L. Bodelier, H. J. Laanbroek, Nitrogen as a regulatory factor of methane oxidation in soils and sediments. *FEMS Microbiol. Ecol.* **47**, 265–277 (2004).
8. P. L. E. Bodelier, A. K. Steenbergh, Interactions between methane and the nitrogen cycle in light of climate change. *Curr. Opin. Environ. Sustain.* **9-10**, 26–36 (2014).
9. L. Y. Stein, R. Roy, P. F. Dunfield, "Aerobic methanotrophy and nitrification: Processes and connections" in *eLS*, J. Battista *et al*., Eds. (Wiley, Chichester, UK, 2012). Available at https://onlinelibrary.wiley.com/doi/full/10.1002/9780470015902.a0022213. Accessed 28 May 2020.
10. L. Y. Stein, The long-term relationship between microbial metabolism and greenhouse gases. *Trends Microbiol.* **28**, 500–511 (2020).
11. M. Monteiro, J. Séneca, C. Magalhães, The history of aerobic ammonia oxidizers: From the first discoveries to today. *J. Microbiol.* **52**, 537–547 (2014).
12. H. Daims, S. Lücker, M. Wagner, A new perspective on microbes formerly known as nitrite-oxidizing bacteria. *Trends Microbiol.* **24**, 699–712 (2016).
13. P. L. Bodelier, P. Frenzel, Contribution of methanotrophic and nitrifying bacteria to CH_4 and NH_4^+ oxidation in the rhizosphere of rice plants as determined by new methods of discrimination. *Appl. Environ. Microbiol.* **65**, 1826–1833 (1999).
14. J. Im, S. W. Lee, L. Bodrossy, M. J. Barcelona, J. D. Semrau, Field application of nitrogen and phenylacetylene to mitigate greenhouse gas emissions from landfill cover soils: Effects on microbial community structure. *Appl. Microbiol. Biotechnol.* **89**, 189–200 (2011).
15. S. W. Lee *et al*., Effect of nutrient and selective inhibitor amendments on methane oxidation, nitrous oxide production, and key gene presence and expression in landfill cover soils: Characterization of the role of methanotrophs, nitrifiers, and denitrifiers. *Appl. Microbiol. Biotechnol.* **85**, 389–403 (2009).
16. K. W. Mandernack *et al*., The biogeochemical controls of N_2O production and emission in landfill cover soils: The role of methanotrophs in the nitrogen cycle. *Environ. Microbiol.* **2**, 298–309 (2000).
17. C. Bédard, R. Knowles, Physiology, biochemistry, and specific inhibitors of CH_4, NH_4^+, and CO oxidation by methanotrophs and nitrifiers. *Microbiol. Rev.* **53**, 68–84 (1989).
18. M. O. Ross, A. C. Rosenzweig, A tale of two methane monooxygenases. *J. Biol. Inorg. Chem.* **22**, 307–319 (2017).
19. A. B. Hooper, T. Vannelli, D. J. Bergmann, D. M. Arciero, Enzymology of the oxidation of ammonia to nitrite by bacteria. *Antonie van Leeuwenhoek* **71**, 59–67 (1997).
20. L. Chistoserdova, Modularity of methylotrophy, revisited. *Environ. Microbiol.* **13**, 2603–2622 (2011).
21. C. Anthony, "Methanol dehydrogenase, a PQQ-containing quinoprotein dehydrogenase" in *Enzyme-Catalyzed Electron and Radical Transfer*, A. Holzenburg, N. S. Scrutton, Eds. (Springer, 2000), pp. 73–117.
22. A. B. Hooper, A. Nason, Characterization of hydroxylamine-cytochrome *c* reductase from the chemoautotrophs *Nitrosomonas europaea* and *Nitrosocystis oceanus*. *J. Biol. Chem.* **240**, 4044–4057 (1965).
23. L. E. Lehtovirta-Morley, Ammonia oxidation: Ecology, physiology, biochemistry and why they must all come together. *FEMS Microbiol. Lett.* **365**, fny058 (2018).
24. K. M. Lancaster, J. D. Caranto, S. H. Majer, M. A. Smith, Alternative bioenergy: Updates to and challenges in nitrification metalloenzymology. *Joule* **2**, 421–441 (2018).
25. A. B. Hooper, K. R. Terry, Hydroxylamine oxidoreductase of *Nitrosomonas*. Production of nitric oxide from hydroxylamine. *Biochim. Biophys. Acta* **571**, 12–20 (1979).
26. P. Cedervall, A. B. Hooper, C. M. Wilmot, Structural studies of hydroxylamine oxidoreductase reveal a unique heme cofactor and a previously unidentified interaction partner. *Biochemistry* **52**, 6211–6218 (2013).
27. W. J. Maalcke *et al*., Structural basis of biological NO generation by octaheme oxidoreductases. *J. Biol. Chem.* **289**, 1228–1242 (2014).
28. M. G. Klotz *et al*., Evolution of an octahaem cytochrome *c* protein family that is key to aerobic and anaerobic ammonia oxidation by bacteria. *Environ. Microbiol.* **10**, 3150–3163 (2008).
29. J. D. Caranto, K. M. Lancaster, Nitric oxide is an obligate bacterial nitrification intermediate produced by hydroxylamine oxidoreductase. *Proc. Natl. Acad. Sci. U.S.A.* **114**, 8217–8222 (2017).
30. J. A. Duine, J. Frank Jr., Studies on methanol dehydrogenase from Hyphomicrobium X. Isolation of an oxidized form of the enzyme. *Biochem. J.* **187**, 213–219 (1980).
31. M. A. Campbell *et al*., Model of the molecular basis for hydroxylamine oxidation and nitrous oxide production in methanotrophic bacteria. *FEMS Microbiol. Lett.* **322**, 82–89 (2011).
32. A. T. Poret-Peterson, J. E. Graham, J. Gulledge, M. G. Klotz, Transcription of nitrification genes by the methane-oxidizing bacterium, *Methylococcus capsulatus* strain Bath. *ISME J.* **2**, 1213–1220 (2008).
33. G. Nyerges, L. Y. Stein, Ammonia cometabolism and product inhibition vary considerably among species of methanotrophic bacteria. *FEMS Microbiol. Lett.* **297**, 131–136 (2009).
34. S. S. Mohammadi, A. Pol, T. van Alen, M. S. M. Jetten, H. J. M. Op den Camp, Ammonia oxidation and nitrite reduction in the verrucomicrobial methanotroph *Methylacidiphilum fumariolicum* SolV. *Front. Microbiol.* **8**, 1901 (2017).
35. G. Nyerges, S. K. Han, L. Y. Stein, Effects of ammonium and nitrite on growth and competitive fitness of cultivated methanotrophic bacteria. *Appl. Environ. Microbiol.* **76**, 5648–5651 (2010).
36. S. Hoefman *et al*., Niche differentiation in nitrogen metabolism among methanotrophs within an operational taxonomic unit. *BMC Microbiol.* **14**, 83 (2014).
37. K. D. Kits, D. J. Campbell, A. R. Rosana, L. Y. Stein, Diverse electron sources support denitrification under hypoxia in the obligate methanotroph *Methylomicrobium album* strain BG8. *Front. Microbiol.* **6**, 1072 (2015).
38. K. D. Kits, M. G. Klotz, L. Y. Stein, Methane oxidation coupled to nitrate reduction under hypoxia by the Gammaproteobacterium *Methylomonas denitrificans*, sp. nov. type strain FJG1. *Environ. Microbiol.* **17**, 3219–3232 (2015).
39. A. Pol *et al*., Methanotrophy below pH 1 by a new Verrucomicrobia species. *Nature* **450**, 874–878 (2007).
40. K. R. Terry, A. B. Hooper, Hydroxylamine oxidoreductase: A 20-heme, 200 000 molecular weight cytochrome *c* with unusual denaturation properties which forms a 63 000 molecular weight monomer after heme removal. *Biochemistry* **20**, 7026–7032 (1981).
41. A. Pol *et al*., Rare earth metals are essential for methanotrophic life in volcanic mudpots. *Environ. Microbiol.* **16**, 255–264 (2014).
42. L. Chistoserdova, M. G. Kalyuzhnaya, Current trends in methylotrophy. *Trends Microbiol.* **26**, 703–714 (2018).
43. J. S. Graf *et al*., Bloom of a denitrifying methanotroph, "*Candidatus* Methylomirabilis limnetica," in a deep stratified lake. *Environ. Microbiol.* **20**, 2598–2614 (2018).
44. W. Versantvoort *et al*., Comparative genomics of *Candidatus* Methylomirabilis species and description of *Ca*. Methylomirabilis lanthanidiphila. *Front. Microbiol.* **9**, 1672 (2018).
45. K. F. Ettwig *et al*., Nitrite-driven anaerobic methane oxidation by oxygenic bacteria. *Nature* **464**, 543–548 (2010).
46. A. F. Khadem, A. Pol, M. S. M. Jetten, H. J. M. Op den Camp, Nitrogen fixation by the verrucomicrobial methanotroph "*Methylacidiphilum fumariolicum*" SolV. *Microbiology* **156**, 1052–1059 (2010).
47. P. L. E. Bodelier, Interactions between nitrogenous fertilizers and methane cycling in wetland and upland soils. *Curr. Opin. Environ. Sustain.* **3**, 379–388 (2011).
48. S. Acton, E. Baggs, Interactions between N application rate, CH_4 oxidation and N_2O production in soil. *Biogeochemistry* **103**, 15–26 (2011).
49. R. A. Schmitz *et al*., The thermoacidophilic methanotroph *Methylacidiphilum fumariolicum* SolV oxidizes subatmospheric H_2 with a high-affinity, membrane-associated [NiFe] hydrogenase. *ISME J.* **14**, 1223–1232 (2020).
50. U. K. Laemmli, Cleavage of structural proteins during the assembly of the head of bacteriophage T4. *Nature* **227**, 680–685 (1970).
51. D. D. Mruk, C. Y. Cheng, Enhanced chemiluminescence (ECL) for routine immunoblotting: An inexpensive alternative to commercially available kits. *Spermatogenesis* **1**, 121–122 (2011).
52. I. Wittig, M. Karas, H. Schägger, High resolution clear native electrophoresis for in-gel functional assays and fluorescence studies of membrane protein complexes. *Mol. Cell. Proteomics* **6**, 1215–1225 (2007).
53. M. H. Farhoud *et al*., Protein complexes in the archaeon *Methanothermobacter thermautotrophicus* analyzed by blue native/SDS-PAGE and mass spectrometry. *Mol. Cell. Proteomics* **4**, 1653–1663 (2005).
54. J. J. Almagro Armenteros *et al*., SignalP 5.0 improves signal peptide predictions using deep neural networks. *Nat. Biotechnol.* **37**, 420–423 (2019).
55. R. C. Edgar, MUSCLE: Multiple sequence alignment with high accuracy and high throughput. *Nucleic Acids Res.* **32**, 1792–1797 (2004).
56. S. Kumar, G. Stecher, M. Li, C. Knyaz, K. Tamura, MEGA X: Molecular evolutionary genetics analysis across computing platforms. *Mol. Biol. Evol.* **35**, 1547–1549 (2018).